JACS
JOURNAL OF THE AMERICAN CHEMICAL SOCIETY
Communication
pubs.acs.org/JACS

Barrierless Photoisomerization of 11-*cis* Retinal Protonated Schiff Base in Solution

Giovanni Bassolino,[†] Tina Sovdat,[‡] Alex Soares Duarte,[†] Jong Min Lim,[†] Christoph Schnedermann,[†] Matz Liebel,[†,§] Barbara Odell,[‡] Timothy D. W. Claridge,[‡] Stephen P. Fletcher,*[,‡] and Philipp Kukura*[,†]

[†]Department of Chemistry, Physical and Theoretical Chemistry Laboratory, University of Oxford, South Parks Road, Oxford OX1 3QZ, U.K.

[‡]Department of Chemistry, Chemistry Research Laboratory, University of Oxford, Mansfield Road, Oxford OX1 3TA, U.K.

Supporting Information

ABSTRACT: A hallmark of the primary visual event is the barrierless, ultrafast, and efficient 11-*cis* to all-*trans* photoisomerization of the retinal protonated Schiff base (RPSB) chromophore. The remarkable reactivity of RPSB in the visual pigment rhodopsin has been attributed to potential energy surface modifications enabled by evolution-optimized chromophore−protein interactions. Here, we use a combined synthetic and ultrafast spectroscopic approach to show that barrierless photoisomerization is an intrinsic property of 11-*cis* RPSB, suggesting that the protein may merely adjust the ratio between fast reactive and slow unreactive decay channels. These results call for a re-evaluation of our understanding and theoretical description of RPSB photochemistry.

Retinal protonated Schiff bases (RPSBs) have become a benchmark system for understanding the origins of efficient and tunable photochemistry. Several decades of experimental and theoretical studies[1−3] have been aimed at unravelling the origins of the difference in photoreactivity of RPSBs in solution with that in a retinylidene protein environment. As an example, 11-*cis* RPSB in rhodopsin (RHO) exhibits a red-shifted absorption maximum (498 nm vs 442 nm),[3,4] a drastically shorter excited state lifetime (~0.05 vs 4 ps)[5−9] and a higher isomerization yield (Φ = 0.65 vs 0.22)[4,10,11] compared to solution. The extreme speed of the photoreaction has been attributed to the ability of the protein to modify the excited electronic state potential energy surface of 11-*cis* RPSB when bound to the opsin apoprotein in such a way that the reaction becomes effectively barrierless.[5,6] This experimentally driven hypothesis was confirmed theoretically[12] and further validated by the comparatively slow excited state decay of 11-*cis* RPSB in solution (4 ps).[7−9] Spectroscopic[7,13] and computational[14−16] evidence proposed the existence of an excited state barrier for RPSB in solution along the isomerization coordinate. In the original three-state model for the isomerization, the barrier was proposed to arise from an avoided crossing between S_1 and S_2 states,[13] and recent computational evidence for a model chromophore supports this notion.[17]

The picosecond excited state dynamics of 11-*cis* and all-*trans* RPSB appear essentially identical (Figure 1a).[7,18] When using high temporal resolution (<30 fs), however, a clear additional signature is evident for 11-*cis* during the first 200 fs after photoexcitation that cannot be explained by a coherent artifact (Figure 1b and Supplementary Figure 2). Although this feature points toward the existence of an additional decay channel for 11-*cis* that is absent for all-*trans* RPSB, it cannot determine its role in photoproduct formation alone. To address the origin of the differences in the ultrafast transient absorption between the two isomers, we employed a combined synthetic and spectroscopic approach.

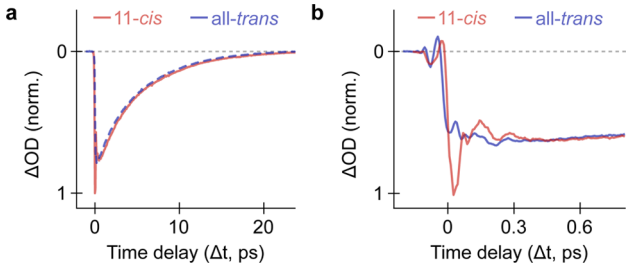

Figure 1. Comparison of RPSB excited state kinetics in solution. (a) Differential transient absorption monitoring the excited state absorption of all-*trans* (blue) and 11-*cis* (red) RPSB in MeOH at 680 nm. (b) Zoom of the first 800 fs of the excited state dynamics. Data were acquired with actinic-probe steps of 60 and 6 fs, respectively.

We have recently shown that the addition of a methyl group to the 10-position of all-*trans* RPSB significantly reduces the excited state lifetime and the isomerization yield.[19] This lead to an extension of the barrier tuning mechanism in solution[20] initially proposed for bacteriorhodopsin (BR), for which no such correlation was observed.[13] Performing the same chemical modification for 11-*cis* RPSB (to produce 10-Me-11-*cis* RPSB, Figure 2a) gave the expected reduction in excited state lifetime (Figure 2b), but with no concomitant decrease in the isomerization yield (Figure 2c). These results suggest that the long-lived excited state population observed in 11-*cis* RPSB (Figure 1a) may not be undergoing isomerization and, in contrast to all-*trans* RPSB, be unreactive.

To monitor the photoproduct formation kinetics directly, we use a multipulse population control approach (Figure 3a), previously applied to all-*trans* RPSB in solution,[21] BR,[22] and RHO.[23] Following electronic excitation by a short actinic pulse (A), the system evolves on the excited state potential energy

Received: June 23, 2015
Published: September 16, 2015

DOI: 10.1021/jacs.5b06492
J. Am. Chem. Soc. 2015, 137, 12434−12437

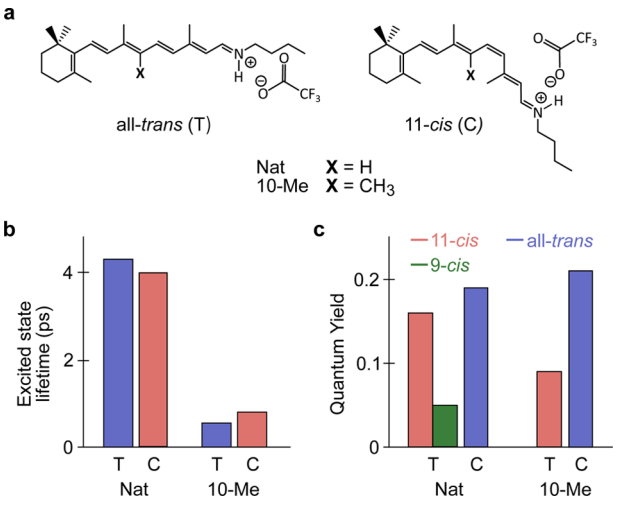

Figure 2. Comparison of modified RPSB dynamics and reactivity in MeOH. (a) Structures of all-*trans* and 11-*cis* derivatives studied in this work. (b,c) Excited state lifetimes and quantum yields for the derivatives shown in (a). Colors in (c) identify the photoproduct formed when irradiating the all-*trans* (T) or 11-*cis* (C) isomer of the different derivatives. Data for all-*trans* isomers of NAT and 10-Me are taken from ref 19.

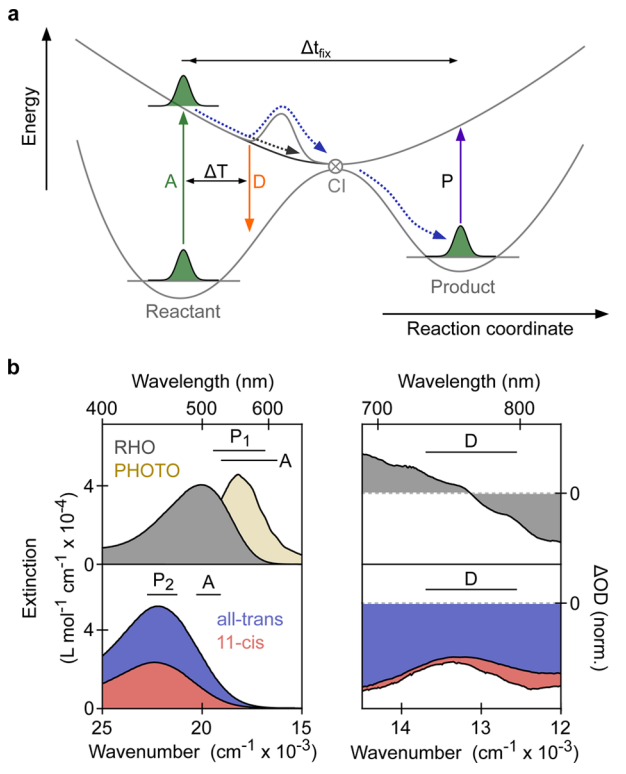

Figure 3. Photophysics of retinal in solution and rhodopsin. (a) Illustration of the reaction coordinate and the actinic-dump-probe scheme. The gray surface includes a barrier in the excited state, while the one shown in black leads to a barrierless excited state decay. The blue and black dotted arrows represent the corresponding trajectories. (b) Absorption spectra of rhodopsin (RHO), photorhodopsin (PHOTO),[5] and 11-*cis* and all-*trans* RPSB in MeOH. The bandwidths of the actinic (A) pulses and the probed spectral region (P_1 and P_2 for RHO and RPSBs in solution, respectively) are indicated by black lines. Transient absorption spectra of RHO and RPSB in solution (11-*cis*, red; all-*trans*, blue) at 80 and 300 fs actinic-probe delays (Δt), respectively. The bandwidth of the dump (D) pulse is indicated as a black line.

surface toward a surface crossing to eventually form the ground state photoproduct or return to the starting material. In a population control experiment, a second short dump (D) pulse, resonant only with electronic transitions originating from the excited state such as stimulated emission or photoinduced absorption, depletes the excited state population before the reaction completes.

For RHO, the primary product photorhodopsin[5] exhibits a significantly shifted ground state absorption maximum compared to the reactant (570 vs 498 nm, Figure 3b). As a result, the reaction kinetics can be monitored by recording the sample absorbance at wavelengths >560 nm where RHO does not absorb significantly (Figure 3b).[5,6] For RPSB in solution, the absorption maxima of all-*trans* and 11-*cis* overlap and are only marginally shifted ($\Delta\lambda \approx 5$ nm),[4] making it impossible to differentiate photoisomerized from unreactive molecules by probing specific spectral ranges as for RHO. The all-*trans* and 11-*cis* isomers, however, exhibit significantly different molar extinction coefficients of 51 800 and 23 300 M^{-1} cm^{-1}, respectively.[4] Isomerization from 11-*cis* to all-*trans* therefore increases the overall sample absorbance near 450 nm and *vice versa*.

The population control experiments were all performed in the same fashion (Figure 3a). The system composition is probed at a fixed actinic-probe time delay (Δt) chosen to ensure that the relevant photochemistry is complete when the probe pulse reaches the sample ($\Delta t = 60$ ps for the solution experiments, $\Delta t =$ 20 ps for RHO). We then monitored changes in the transient absorbance as a function of the actinic-dump time delay (ΔT − 300 to +4000 fs for RPSBs in solution, and −300 to +1500 fs for RHO). The dump pulse is centered at 780 nm in all cases, matching the transient stimulated emission characteristic of the excited electronic state (Figure 3b) while ensuring that the depletion operates in the linear regime (Supplementary Figure 10). With this experimental approach, a dump-induced difference in the isomerization yield manifests itself as a change in the transient absorbance at the probed Δt delay. As we are measuring a difference in a transient absorption signal, which in itself is a differential optical density ($OD_{actinicON} - OD_{actinicOFF}$), the resulting signal corresponds to a double differential measurement of the optical density of the sample ($\Delta\Delta OD$).

Since the isomerization of all-*trans* to 11-*cis* RPSB converts a fraction of a higher absorbing species ($\varepsilon_{atr} = 51\,800\ M^{-1}\ cm^{-1}$) to a lower absorbing one ($\varepsilon_{cis} = 23\,300\ M^{-1}\ cm^{-1}$), it leads to a decrease of the overall absorbance near 450 nm at long actinic-probe delays as the isomerization completes. If the NIR dump pulse acts to decrease the amount of photoproduct formed (Φ) it results in $\Delta\Delta OD > 0$ ($\Phi_D < \Phi_0$, Figure 4). The opposite is true if the dump generates additional photoproduct ($\Phi_D > \Phi_0$).

For all-*trans* RPSB (blue, Figure 4), we observe a negative $\Delta\Delta OD$ at early actinic-dump delays ($\Delta T < 200$ fs), indicating an increased isomerization yield resulting from the interaction with the dump pulse. Within 100 fs, the double differential signal evolves to an approximately equal magnitude but opposite sign, indicative of a decrease in photoproduct formation induced by the dump. The efficacy of the dump in changing the isomerization yield then decays on a time scale matching the excited state lifetime (Figure 1a) in agreement with previous reports.[21] The negative spike at early positive time delays is most likely caused by a secondary excitation due to the absorption of a dump photon after photoexcitation, which enhances the yield of 11-*cis* through the involvement of higher lying electronic states.[24]

DOI: 10.1021/jacs.5b06492
J. Am. Chem. Soc. 2015, 137, 12434−12437

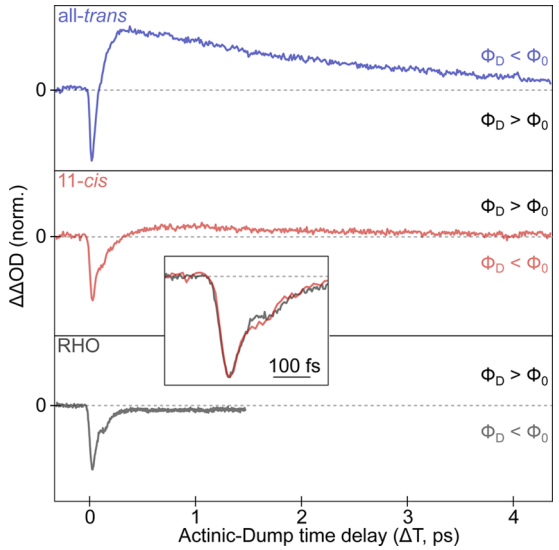

Figure 4. Population control traces for RPSB in solution and rhodopsin. All traces have been normalized with respect to the amplitude of the maximum dumped signal and have been aligned to yield the same rise providing relative time axes in agreement with previously published population control experiments.[21,23] Inset: Zoom of the overlaid dynamics for 11-*cis* RPSB in solution and in RHO.

Despite the similarity of the transient absorption dynamics between 11-*cis* and all-*trans* RPSB in solution, the corresponding action traces are very different. Photoproduct generation for 11-*cis* (red, Figure 4) is only inhibited at early actinic-dump delays (ΔT < 300 fs), with slightly increased product generation at longer time delays, which decayed on a similar time scale as the excited state lifetime. The corresponding action trace for RHO revealed a similar appearance except at long time delays (>0.5 ps), where a small long-term offset corresponding to a decreased photoproduct yield persisted. The action trace for RHO (gray, Figure 4) agrees with expectations from transient absorption[5,6] and previous population control experiments[23] since the dump has a negligible effect on the photoproduct formation for actinic-dump delays >300 fs. The incomplete recovery of the signal approaching a small offset is likely due to partial back-reversion of photorhodopsin, as the red edge of its absorption spectrum overlaps with the spectral coverage of the dump.[25]

Zooming in on the action traces at ΔT < 300 fs reveals an almost perfect overlap between the dynamics of 11-*cis* RPSB in solution and in RHO (Figure 4, inset). The dump reaches maximal efficiency in changing the photochemical outcome at ΔT = 50 fs, almost within the cross-correlation of the actinic and the dump pulses. This behavior is in striking contrast to all-*trans* RPSB, where the maximum efficiency in terms of quenching the photoisomerization is reached at a ∼300 fs delay, before decaying on the picosecond time scale. Furthermore, the decay of the negative ΔΔOD signal completes on the same time scale as the one measured for RHO.

We argue that the ultrafast decay of the action trace for 11-*cis* cannot be explained by a competition between different channels generated by simultaneous photoinduced absorption and stimulated emission following interaction with the dump pulse for the following reasons: (1) Our backbone substitution experiments (Figure 2) suggest that the isomerization does not originate from the long-lived excited state population. (2) In 11-*cis* a long-lived excited state population is present that is lacking in RHO, yet 11-*cis* and RHO exhibit very similar traces in the population control experiment. (3) The transient absorption traces shown in Figure 1 reveal the existence of an ultrafast decay channel in 11-*cis*, which is absent for all-*trans*.

Our observations therefore strongly suggest that the isomerization coordinates for 11-*cis* RPSB in solution and RHO are both barrierless. The topography of the isomerization coordinate toward the conical intersection is thus much more similar in these two very different environments than currently envisioned.[7,8,26−29] The action traces confirm the hypothesis emerging from comparing the dynamics of the methylated isomers (Figure 2) that the long-lived population generating the stimulated emission and fluorescence[7,8] in 11-*cis* RPSB belongs to unreactive, nonisomerizing species. This is in contrast to what has been observed for all-*trans* RPSB[20−22] and suggests that optimized electronic or steric interactions with the protein pocket in rhodopsin are not essential for a rapid and barrierless reaction.[7,8,26−29]

The slight positive ΔΔOD at longer ΔT for 11-*cis* (>0.4 ps) indicates the production of a more absorbing species in the presence of the dump, i.e., an increased yield of the all-*trans* isomer. This behavior could be attributed to two possible mechanisms: absorption of dump photons by hot, unreactive molecules or sequential two-photon absorption of the actinic and dump pulses. We believe that the latter mechanism is more likely due to the absence of a near-infrared absorption of unreactive ground state molecules in the transient absorption. In the presence of the dump, partially resonant with the 750 nm excited state absorption band, the long-lived excited state population could be excited to a higher electronic state from which the system can evolve toward a successfully isomerizing reaction coordinate (see SI).

These results challenge our understanding not only of RPSB reactivity in solution, but more importantly of the likely role of the protein environment in the visual opsins. The population control approach reported here shows that the isomerization dynamics in solution for 11-*cis* RPSB almost perfectly match the time scales of photoproduct formation in RHO. This suggests that ultrafast and barrierless photoisomerization is an intrinsic feature of 11-*cis* RPSB dynamics, irrespective of its environment. The role of the protein may thus be as simple as changing the ratio between molecules taking the ultrafast reactive decay path and those following slower, unreactive trajectories, without significantly affecting the topography of the reaction coordinate. As the differences in the absorption maxima between gas phase, the protein pocket, and solution suggest, the different environments significantly tune the ground to excited state energy gap through electrostatic interactions.[30,31] The data presented here suggest that, notwithstanding the magnitude of the absorption changes, the topography of the reaction coordinate in solution and in rhodopsin may only be weakly affected.

Our results do not provide direct insight into the mechanism underlying the path selection in the protein, but some considerations can still be made. The significantly lower quantum yield in solution has two possible causes: either the photoproduct formation efficiency at the conical intersection is much lower in solution than in the protein, or the ratio of molecules following unreactive and reactive decay channels differs. For the former, the ultrafast channel would still be predominant in solution, and the role of the protein would be to change the photoproduct formation efficiency at the conical intersection. For the latter, the protein would increase the proportion of molecules following the reactive pathway.

DOI: 10.1021/jacs.5b06492
J. Am. Chem. Soc. 2015, 137, 12434−12437

Based on the evidence presented here that reactive excited state dynamics for 11-*cis* RPSB in solution and in RHO are effectively identical, it is reasonable that the changes to the potential energy surface induced by the protein pocket are small apart from the opsin shift. It is well-known that 11-*cis* retinal in solution exists in two major conformers, 12-*s*-*cis* and 12-*s*-*trans*.[32] We used nuclear Overhauser effect (NOE) spectroscopy in MeOD solution to show that the same is true for 11-*cis* RPSB (see SI). As 12-*s*-*trans* is the conformation assumed by retinal in the protein,[33−35] we evaluated the conformer ratio for RPSB in MeOD through a series of transient NOE measurements and found it to be approximately 50:50 (see SI). Assuming that only the 12-*s*-*trans* protein-like conformer is reactive with a QY of 0.65 (same as RHO) results in an estimate of the solution QY of 0.33 ± 0.06, surprisingly close to the measured value of 0.19 ± 0.04 considering the number of approximations required (see SI).

We therefore propose that the differences in reactivity for 11-*cis* RPSB in solution and protein may be largely due to preselection of the more reactive conformer by the protein with the ensuing dynamics and quantum yield almost unaltered. In this scenario, the choice between the ultrafast reactive channel and the long-lived unreactive one would be a function of the molecular conformation at the moment of excitation, i.e., in the ground electronic state.[36] This hypothesis is supported by recent computational studies on model systems, which have found the photoisomerization outcome to depend on the starting geometry.[37]

■ ASSOCIATED CONTENT

Supporting Information

The Supporting Information is available free of charge on the ACS Publications website at DOI: 10.1021/jacs.5b06492. The data underpinning the results presented in this manuscript can be accessed free of charge at http://ora.ox.ac.uk.

Synthetic schemes and characterization data for the compounds, transient absorption data, ^{1}H NMR of the irradiation experiments, and 11-*cis* RPSB NOE measurements (PDF)

■ AUTHOR INFORMATION

Corresponding Authors

*philipp.kukura@chem.ox.ac.uk
*stephen.fletcher@chem.ox.ac.uk

Present Address

§ICFO, Institut de Ciencies Fotoniques, Mediterranean Technology Park, 08860 Castelldefels, Barcelona, Spain.

Notes

The authors declare no competing financial interest.

■ ACKNOWLEDGMENTS

The authors would like to acknowledge Dr. Rosalie Crouch and the National Eye Institute, National Institutes of Health for a generous donation of 11-*cis* retinal and the use of the University of Oxford Advanced Research Computing (ARC) facility in carrying out this work. The work was supported by the EPSRC (EP/K006630/1).

■ REFERENCES

(1) Kandori, H.; Shichida, Y.; Yoshizawa, T. *Biochemistry* **2001**, *66*, 1197.
(2) Wand, A.; Gdor, I.; Zhu, J.; Sheves, M.; Ruhman, S.; Johnson, M.; Martinez, T. *Annu. Rev. Phys. Chem.* **2013**, *64*, 437.
(3) Ernst, O.; Lodowski, D.; Elstner, M.; Hegemann, P.; Brown, L.; Kandori, H. *Chem. Rev.* **2014**, *114*, 126.
(4) Freedman, K.; Becker, R. S. *J. Am. Chem. Soc.* **1986**, *108*, 1245.
(5) Schoenlein, R. W.; Peteanu, L. A.; Mathies, R. A.; Shank, C. V. *Science* **1991**, *254*, 412.
(6) Peteanu, L. A.; Schoenlein, R. W.; Wang, Q.; Mathies, R. A.; Shank, C. V. *Proc. Natl. Acad. Sci. U. S. A.* **1993**, *90*, 11762.
(7) Kandori, H.; Katsuta, Y.; Ito, M.; Sasabe, H. *J. Am. Chem. Soc.* **1995**, *117*, 2669.
(8) Huppert, D.; Rentzepis, P. M. *J. Phys. Chem.* **1986**, *90*, 2813.
(9) Becker, R. S.; Freedman, K.; Hutchinson, J. A.; Noe, L. J. *J. Am. Chem. Soc.* **1985**, *107*, 3942.
(10) Kim, J. E.; Tauber, M. J.; Mathies, R. A. *Biochemistry* **2001**, *40*, 13774.
(11) Koyama, Y.; Kubo, K.; Komori, M.; Yasuda, H.; Mukai, Y. *Photochem. Photobiol.* **1991**, *54*, 433.
(12) Cembran, A.; Bernardi, F.; Olivucci, M.; Garavelli, M. *Proc. Natl. Acad. Sci. U. S. A.* **2005**, *102*, 6255.
(13) Gai, F.; Hasson, K. C.; McDonald, J. C.; Anfinrud, P. A. *Science* **1998**, *279*, 1886.
(14) Valsson, O.; Filippi, C. *J. Chem. Theory Comput.* **2010**, *6*, 1275.
(15) Gozem, S.; Melaccio, F.; Lindh, R.; Krylov, A. I.; Granovsky, A. A.; Angeli, C.; Olivucci, M. *J. Chem. Theory Comput.* **2013**, *9*, 4495.
(16) Zhou, P.; Liu, J.; Han, K.; He, G. *J. Comput. Chem.* **2014**, *35*, 109.
(17) Muñoz-Losa, A.; Fdez Galván, I.; Aguilar, M. A.; Martín, M. E. *J. Chem. Theory Comput.* **2013**, *9*, 1548.
(18) Kandori, H.; Sasabe, H. *Chem. Phys. Lett.* **1993**, *216*, 126.
(19) Sovdat, T.; Bassolino, G.; Liebel, M.; Schnedermann, C.; Fletcher, S. P.; Kukura, P. *J. Am. Chem. Soc.* **2012**, *134*, 8318.
(20) Bassolino, G.; Sovdat, T.; Liebel, M.; Schnedermann, C.; Odell, B.; Claridge, T. D. W.; Kukura, P.; Fletcher, S. P. *J. Am. Chem. Soc.* **2014**, *136*, 2650.
(21) Zgrablic, G.; Novello, A. M.; Parmigiani, F. *J. Am. Chem. Soc.* **2012**, *134*, 955.
(22) Ruhman, S.; Hou, B.; Friedman, N.; Ottolenghi, M.; Sheves, M. *J. Am. Chem. Soc.* **2002**, *124*, 8854.
(23) Yan, M.; Rothberg, L.; Callender, R. *J. Phys. Chem. B* **2001**, *105*, 856.
(24) Bismuth, O.; Friedman, N.; Sheves, M.; Ruhman, S. *Chem. Phys.* **2007**, *341*, 267.
(25) Mozgovaya, M. N.; Smitienko, O. A.; Shelaev, I. V.; Gostev, F. E.; Feldman, T. B.; Nadtochenko, V. A.; Sarkisov, O. M.; Ostrovsky, M. A. *Dokl. Biochem. Biophys.* **2010**, *435*, 302.
(26) Garavelli, M.; Celani, P.; Bernardi, F.; Robb, M. A.; Olivucci, M. *J. Am. Chem. Soc.* **1997**, *119*, 6891.
(27) Gonzalez-Luque, R.; Garavelli, M.; Bernardi, F.; Merchan, M.; Robb, M. A.; Olivucci, M. *Proc. Natl. Acad. Sci. U. S. A.* **2000**, *97*, 9379.
(28) Kochendoerfer, G. G.; Verdegem, P. J.; van der Hoef, I.; Lugtenburg, J.; Mathies, R. A. *Biochemistry* **1996**, *35*, 16230.
(29) Cembran, A.; Bernardi, F.; Olivucci, M.; Garavelli, M. *J. Am. Chem. Soc.* **2004**, *126*, 16018.
(30) Andersen, L. H.; Nielsen, I. B.; Kristensen, M. B.; El Ghazaly, M. O. A.; Haacke, S.; Nielsen, M. B.; Petersen, M. Å. *J. Am. Chem. Soc.* **2005**, *127*, 12347.
(31) Rajput, J.; Rahbek, D. B.; Andersen, L. H.; Hirshfeld, A.; Sheves, M.; Altoè, P.; Orlandi, G.; Garavelli, M. *Angew. Chem., Int. Ed.* **2010**, *49*, 1790.
(32) Rowan, R.; Warshel, A.; Sykes, B. D.; Karplus, M. *Biochemistry* **1974**, *13*, 970.
(33) Callender, R. H.; Doukas, A.; Crouch, R.; Nakanishi, K. *Biochemistry* **1976**, *15*, 1621.
(34) Palczewski, K.; Kumasaka, T.; Hori, T.; Behnke, C. A.; Motoshima, H.; Fox, B. A.; Le Trong, I.; Teller, D. C.; Okada, T.; Stenkamp, R. E.; Yamamoto, M.; Miyano, M. *Science* **2000**, *289*, 739.
(35) Sugihara, M.; Buss, V.; Entel, P.; Elstner, M.; Frauenheim, T. *Biochemistry* **2002**, *41*, 15259.
(36) Fuss, W. *J. Photochem. Photobiol., A* **2015**, *297*, 45.
(37) Vukovic, L.; Burmeister, C. F.; Kral, P.; Groenhof, G. *J. Phys. Chem. Lett.* **2013**, *4*, 1005.

DOI: 10.1021/jacs.5b06492
J. Am. Chem. Soc. 2015, 137, 12434−12437